

Phonon Density of States in MgB₂

R. Osborn,¹ E. A. Goremychkin,^{1,2} A. I. Kolesnikov,² and D. G. Hinks¹

¹Materials Science Division, Argonne National Laboratory, Argonne, Illinois 60439

²Intense Pulsed Neutron Source, Argonne National Laboratory, Argonne, Illinois 60439

(Received 2 March 2001; published 15 June 2001)

We report inelastic neutron scattering measurements of the phonon density of states in Mg¹¹B₂, which has a superconducting transition at 39.2 K. The acoustic phonons extend in energy to 36 meV, and there are highly dispersive optic branches peaking at 54, 78, 89, and 97 meV. A simple Born–von Kàrmàn model reproduces the mode energies, and provides an estimate of the electron-phonon coupling of $\lambda \sim 0.9$. Furthermore, the estimated boron and magnesium contributions to the isotope effect are in qualitative agreement with experiment. The data confirm that a conventional phonon mechanism, with moderately strong electron-phonon coupling, can explain the observed superconductivity.

DOI: 10.1103/PhysRevLett.87.017005

PACS numbers: 74.25.Kc, 63.20.Kr, 74.62.–c, 78.70.Nx

There has already been rapid progress in our understanding of the properties of MgB₂, since the first announcement of superconductivity with a critical temperature of 39 K [1]. Although some have speculated that the high value of T_c must require a novel mechanism for superconductivity [2], initial experimental reports suggest that a conventional phonon mechanism is sufficient. Both the observation of the isotope effect [3,4] and a simple BCS form for the energy gap measured by point-contact tunneling [5] are consistent with phonon-mediated superconductivity, with the high transition temperature made possible by the high frequency of boron vibrational modes. Initial estimates of phonon frequencies, from electronic structure calculations [6–8], predict that they are consistent with the observed critical temperature, although An *et al.* [7] and Kong *et al.* [8] predict that only a few modes have significant electron-phonon coupling.

The strength and frequency dependence of the electron-phonon coupling is determined by measurements of both the electron-phonon spectral density, $\alpha^2(\omega)F(\omega)$, and the bare phonon density of states (PDOS), $F(\omega)$. $\alpha^2(\omega)F(\omega)$ can be derived by inversion of tunneling data, while $F(\omega)$ is derived from measurements of the inelastic neutron scattering law $S(Q, \omega)$. In systems where both sets of data are available, $\alpha(\omega)$ usually varies smoothly with frequency so the bare PDOS provides useful estimates of the frequency moments that determine T_c [9].

We report measurements of the phonon density of states on an isotopically enriched polycrystalline sample of Mg¹¹B₂ [10] using time-of-flight neutron spectroscopy at the Intense Pulsed Neutron Source, Argonne National Laboratory. They confirm that boron vibrational frequencies extend as high as 100 meV. The acoustic modes peak at 36 meV, while there are dispersive optic branches at 54, 78, 89, and 97 meV, in good agreement with predictions based on electronic structure calculations [6–8]. A simple Born–von Kàrmàn (BvK) model, which reproduces the energies of the main spectral features, is used to determine the logarithmic frequency moment of the PDOS, which provides a preliminary estimate of the electron-phonon

coupling, $\lambda \sim 0.9$ (assuming $\mu^* = 0.1$). We also predict the scale of PDOS shifts with isotopic mass, providing estimates of the magnesium and boron contributions to the isotope effect. Given the uncertainties in this analysis, the agreement with experiment is satisfactory, and allows us to conclude that the superconductivity is consistent with a conventional phonon mechanism with moderately strong electron-phonon coupling.

The MgB₂ sample was synthesized from a high purity, 3 mm diameter Mg rod and isotopic ¹¹B (Eagle Picher, 98.46 at. % ¹¹B). The Mg rod was cut into pieces about 4 mm long and mixed with the 200 mesh ¹¹B powder. The reaction was done under moderate pressure (50 bars) of UHP argon at 850 °C. At this temperature the gas-solid reaction was complete in about one hour. The sample (approximately 20 g) was contained in a 30 ml tantalum crucible with a closely fitting cover. There was surface reaction between the Ta crucible and the reactants at the synthesis temperature but the products of this reaction could be mechanically removed. X-ray diffraction showed some small, unidentified impurity peaks in the resultant powder, but the impurity concentration is too small to affect the PDOS measurements.

The neutron scattering experiments were performed on the low resolution medium energy chopper spectrometer (LRMECS), using fixed incident energies of 200, 130, and 50 meV. LRMECS has continuous detector coverage with scattering angles from 2.4° to 117.5° so that a broad range of wave vector transfers, Q , are measured simultaneously, e.g., $2 \leq Q \leq 12 \text{ \AA}^{-1}$ at an energy transfer, $\omega = 60 \text{ meV}$. This is extremely important in accurate determinations of the PDOS when the scattering is predominantly coherent, as it is in Mg¹¹B₂. The coherent (incoherent) scattering cross sections are 3.63 b (0.08 b) and 5.56 b (0.21 b) for Mg and ¹¹B, respectively. Unless the scattering is purely incoherent, it is necessary to average the measured neutron scattering over a large volume of reciprocal space in order for the resulting measurements to reflect the true phonon density of states.

The neutron data taken with an incident energy of 200 meV shows that the PDOS extends up to 100 meV. Above that energy, the scattering comprises only a broad multiphonon tail. Figure 1 shows data taken at 130 meV at 8 K. The peak in the acoustic PDOS occurs at about 36 meV, while there are broad optic bands at 54, 78, 89, and 97 meV. The spectrometer resolution decreases with energy transfer from 5.9 meV at $\omega = 40$ to 3.4 meV at $\omega = 90$ meV. The large width of these features is not just a resolution effect, but arises from dispersion of the optic phonon branches. We have also performed measurements at 30, 50, and 100 K. The only statistically significant difference between these temperatures is a small suppression of the peak at 54 meV below T_c . In a polycrystalline average, this is a very small effect, but it could still represent a significant change in an individual phonon branch. Interestingly, this is the mode that An and Pickett predict to have the strongest electron-phonon coupling [7], but such con-

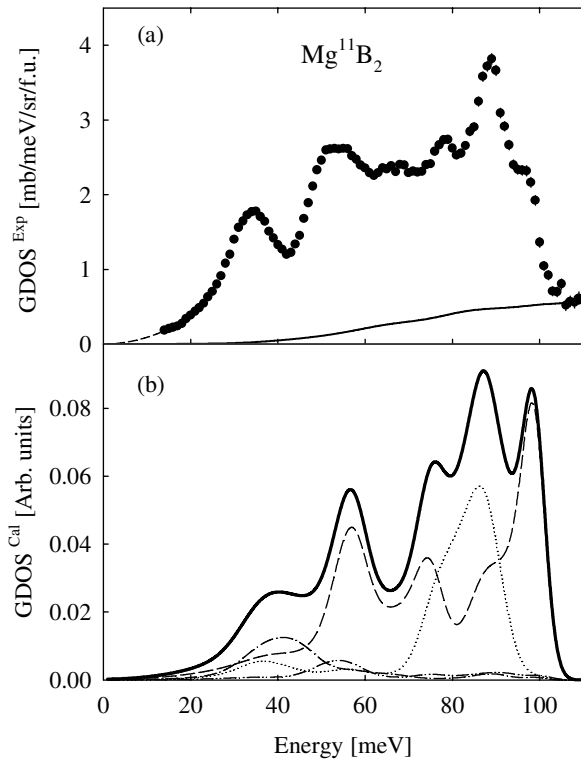


FIG. 1. (a) The generalized phonon density of states, $\text{GDOS} = \sum_{i=\text{Mg,B}} \sigma_i \exp(-2W_i) G_i(\omega) / M_i$, determined from the inelastic neutron scattering spectrum of MgB_2 measured on LRMECS at 8 K with an incident neutron energy 130 meV integrated over wave vectors from 9 to 12 \AA^{-1} . The solid line is the estimated multiphonon contribution. (b) The calculated GDOS based on the BvK model described in the text convoluted with the resolution function of the spectrometer. The dashed lines represent the projections of the partial contributions to GDOS; the in-plane boron modes (long-dashed line), out-of-plane boron modes (dotted line), in-plane magnesium modes (dash-dotted line), and out-of-plane magnesium modes (dash-double-dotted line).

clusions need to await single crystal phonon dispersion measurements.

We see no evidence of the peak at 17 meV reported by Sato *et al.* [11]. They used a different scattering geometry to LRMECS with a fixed scattered neutron energy of 4.59 meV. Consequently, their PDOS is derived from measurements along a relatively narrow (Q, ω) trajectory, with ω quadratically coupled to Q . This can produce a reasonable approximation to the PDOS at high Q and ω where the polycrystalline averaging ensures integration over a large number of Brillouin zones, but the approximation is less reliable at low Q and ω . Figure 2 shows that there are a number of peaks, e.g., at $Q = 2.7 \text{ \AA}^{-1}$, in a constant-energy cut through the LRMECS data with $\omega \approx 17$ meV. The Q dependence of coherent neutron scattering from acoustic phonons in a polycrystal should be approximately proportional to $Q^2 S(Q, \omega = 0)$ [12], a prediction supported by comparison with the calculated $S(Q, 0)$ in Fig. 2. In a coupled (Q, ω) scan, such peaks in Q could be misinterpreted as peaks in $F(\omega)$ [13].

In a multicomponent system, the inelastic neutron scattering law in polycrystalline samples is given by

$$S(Q, \omega) = \sum_{i=\text{Mg,B}} \sigma_i \frac{\hbar Q^2}{2M_i} \exp(-2W_i) \times \frac{G_i(\omega)}{\omega} [n(\omega) + 1], \quad (1)$$

where σ_i and M_i are the neutron scattering cross section and atomic mass of the i th atom and $n(\omega) = [\exp(\hbar\omega/k_B T) - 1]^{-1}$ is the Bose population factor. The weighted PDOS, $G(\omega) = \sum_i G_i(\omega)$, where $G_i(\omega)$ is defined as

$$G_i(\omega) = \frac{1}{3N} \sum_{j\mathbf{q}} |\mathbf{e}_i(j, \mathbf{q})|^2 \delta[\omega - \omega(j, \mathbf{q})], \quad (2)$$

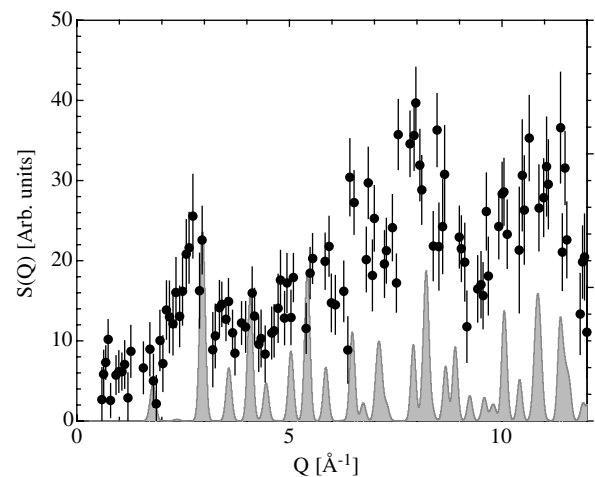


FIG. 2. $S(Q)$ determined from a constant-energy cut through the LRMECS data measured at 8 K with an incident energy of 130 meV. The data are summed over energy transfers of 15 to 18 meV. The shaded peaks are $S(Q)$ at $\omega = 0$ calculated using the known structure of MgB_2 .

which, in turn, defines the Debye-Waller factor, $W_i(Q)$ through

$$W_i(Q) = \frac{\hbar Q^2}{2M_i} \int_0^\infty \frac{G_i(\omega)}{\omega} [2n(\omega) + 1]. \quad (3)$$

$\omega(j, \mathbf{q})$ and $e_i(j, \mathbf{q})$ are the frequencies and eigenvectors, respectively, of the phonon modes. Because the Mg and B partial contributions are weighted by σ/M , the measured spectrum does not represent the true PDOS, although the stronger cross section and lighter mass of the boron atoms ensure that they make the dominant contribution.

We have analyzed the data in terms of a simple BvK model that is sufficient to describe the principal features. MgB_2 has a hexagonal structure with the lattice parameters $a = 3.082 \text{ \AA}$ and $c = 3.515 \text{ \AA}$ [14]. The lattice is composed of a honeycomb of B atoms separated by hexagonal Mg layers, leading to comparisons with graphite intercalation compounds [7]. The nearest-neighbor distances are 3.082 and 3.515 \AA for Mg-Mg pairs in the basal plane and along the c axis, respectively, 2.501 \AA for Mg-B pairs, and 1.780 and 3.515 \AA for B-B pairs in the basal plane and along the c axis, respectively.

Assuming central forces, each atom-atom interaction can be represented by two parameters, the longitudinal and transverse force constants. We have included only nearest-neighbor interactions between Mg-Mg and B-B atoms in the basal plane and along the c axis, and between Mg-B pairs in neighboring layers. The results of the calculation, which was performed using the UNISOFT program [15], are shown in Fig. 1(b), where the in-plane and out-of-plane projections of the partial contributions to the generalized PDOS from boron and magnesium modes are also plotted.

It is possible to reproduce the frequencies of the peaks in the PDOS with only six force constants. These are the longitudinal and transverse in-plane B-B interactions (90 and 7.5 N/m, respectively), the longitudinal out-of-plane B-B interaction (20 N/m), the longitudinal in-plane and out-of-plane Mg-Mg interactions (both 0.6 N/m), and the longitudinal and transverse Mg-B interactions (70 and 2 N/m, respectively). The remaining transverse nearest-neighbor interactions had a negligible effect on the mode frequencies.

The frequencies of the main peaks in the PDOS are well represented by this model, but it is clear that the widths of the peaks are not; i.e., we have underestimated the dispersion of the optic branches. It would be possible to improve the agreement by the introduction of additional parameters representing longer-range interactions, but the results of such an analysis would be meaningless at the present time. Complete measurements of the phonon dispersion on single crystals would allow the model to be refined, but the present analysis is sufficient to provide good estimates of the frequency moments of the PDOS that determine the phonon contribution to T_c .

Figure 3 shows the resulting bare PDOS, $F(\omega)$, defined as

$$F(\omega) = \frac{1}{N} \sum_{j\mathbf{q}} \delta[\omega - \omega(j, \mathbf{q})]. \quad (4)$$

This is similar to Eq. (2) but does not include the vibrational eigenvectors. In a Bravais lattice, the two quantities are equivalent, but in multicomponent systems with very different atomic masses, $G(\omega)$ will tend to weight the PDOS to higher frequencies because of the smaller atomic displacements of the heavier atoms.

We now discuss the implications of this data for understanding the superconducting transition temperature. This may be estimated using the Allen-Dynes equation [16]

$$k_B T_c = \frac{\hbar \omega_{\text{ln}}}{1.2} \exp\left[-\frac{1.04(1 + \lambda)}{\lambda - \mu^*(1 + 0.62\lambda)}\right], \quad (5)$$

where λ is the electron-phonon coupling, μ^* is the Coulomb repulsion, and ω_{ln} is the logarithmic phonon average energy defined in Eq. 2.16 of Ref. [9]. ω_{ln} is an average over $\alpha^2(\omega)F(\omega)$, so we need to make the assumption that $\alpha(\omega)$ is approximately energy independent, in which case it cancels from the equation. We have a choice of two functions to use. It is more conventional to use the bare PDOS, $F(\omega)$, given by Eq. (4). However, this function fails to take into account the size of the atomic displacements of the different phonon modes; they are included in $G(\omega)$. The electron-phonon matrix elements contain the product of the mode eigenvectors and the gradient of the crystal potential [8], so it is likely that $G(\omega)$ represents a better approximation to $\alpha^2(\omega)F(\omega)$.

The Allen-Dynes equation can be inverted to estimate the value of λ for a given value of T_c and μ^* . From integrating over the model calculation of $G(\omega)$, we estimate that ω_{ln} is 57.9 meV [53.8 meV when determined

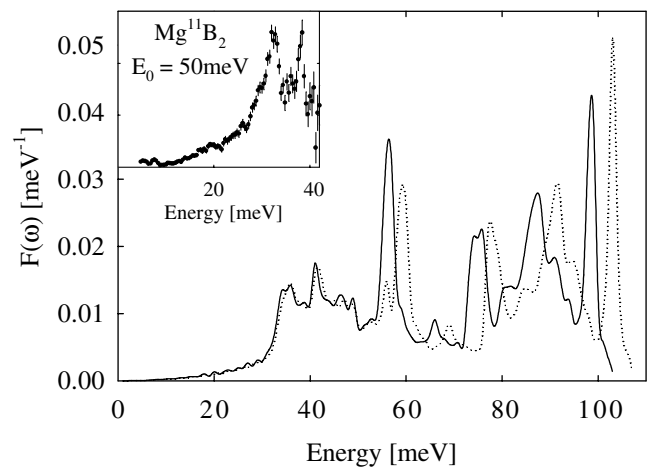


FIG. 3. The bare phonon density of states, $F(\omega)$, of Mg^{11}B_2 (solid line) and Mg^{10}B_2 (dotted line), calculated from the BvK model described in the text (normalized to 1.0). The inset shows neutron data taken with an incident energy of 50 meV showing the split peaks in the acoustic density of state.

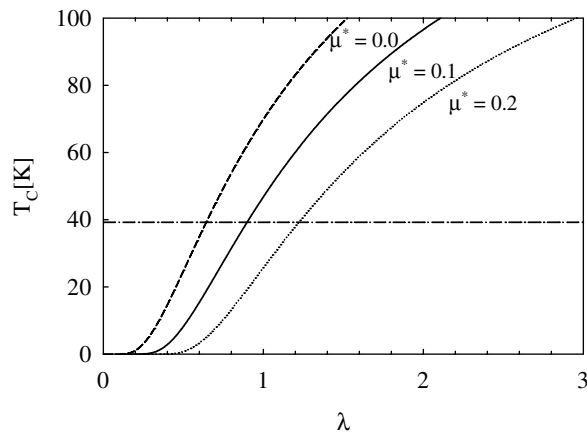


FIG. 4. Variation of the superconducting transition temperature with λ using the Allen-Dynes equation and the value of the logarithmic phonon average, $\omega_{\ln} = 57.9$ meV, determined from the $G(\omega)$. Three values of the Coulomb repulsion, $\mu^* = 0.0$ (dashed line), 0.1 (solid line), and 0.2 (dotted line), are plotted. The dash-dotted line is the measured value of T_c in Mg^{11}B_2 .

from $F(\omega)$]. Figure 4 shows calculations of T_c using three typical values of μ^* compared to the measured value of Mg^{11}B_2 . This shows that the measured value of T_c is consistent with a phonon mechanism with values of λ in the range 0.6 to 1.2. $\lambda = 0.9$ at the most frequently cited value of $\mu^* = 0.1$. ω_{\ln} nearly coincides with the energy of the E_{2g} mode that An and Pickett predict will dominate the electron-phonon coupling [7]. It is impossible to determine, on the basis of our measurements, whether the entire phonon spectrum is involved in the superconductivity or only a subset that occurs close to the average energy.

Finally, we can use the BvK model to calculate the isotope effect. The dotted line in Fig. 3 shows a calculation of the PDOS in Mg^{10}B_2 , illustrating the significant energy shifts in all the high frequency boron modes. Substituting ^{26}Mg for ^{24}Mg produces much smaller shifts. The total isotope coefficient is given by the sum of the partial isotope coefficients, $\beta = \sum_{i=\text{Mg,B}} \beta_i$, where $\beta_i = -\delta \ln T_c / \delta \ln M_i = -\delta \ln \omega_{\ln} / \delta \ln M_i$ and should be close to 0.5 with our estimates of λ [9]. If we use $G(\omega)$ to calculate β_B and β_{Mg} , we obtain values of 0.42 and 0.08, respectively, compared to the experimentally determined values of ~ 0.3 [3,4] and ~ 0.02 [4], respectively. Therefore, even if all the phonon modes are involved in the pairing interactions, we estimate that the boron contribution to the isotope effect is 5 times larger than the magnesium

contribution. The experimental ratio is even greater, which suggests that one or more boron modes have an enhanced electron-phonon coupling. We cannot explain, from our measurements alone, why the experimental value of β is significantly lower than 0.5; this is discussed in Ref. [4].

In conclusion, we have measured the phonon density of states in Mg^{11}B_2 , and used the data to produce a simple BvK force-constant model of the vibrational spectra. Our analysis allows us to conclude that the measured values of the transition temperature and the isotope effect are consistent with a conventional phonon mechanism for the superconductivity with moderately strong electron-phonon coupling. It will be extremely useful to compare our data with tunneling measurements of the electron-phonon spectral density, in order to determine whether the whole phonon spectrum is involved in the superconductivity, or only a few specific modes.

This work was supported by the U.S. DOE Office of Science under Contract No. W-31-109-ENG-38.

- [1] J. Nagamatsu *et al.*, Nature (London) **410**, 63 (2001).
- [2] J. E. Hirsch, Phys. Lett. A **282**, 392 (2001).
- [3] S. L. Bud'ko *et al.*, Phys. Rev. Lett. **86**, 1877 (2001).
- [4] D. G. Hinks, H. Claus, and J. D. Jorgensen, Nature (London) **411**, 457 (2001).
- [5] H. Schmidt *et al.*, Phys. Rev. B **63**, 220504(R) (2001); see also G. Karapetrov *et al.*, Phys. Rev. Lett. **86**, 4374 (2001).
- [6] J. Kortus *et al.*, Phys. Rev. Lett. **86**, 4656 (2001).
- [7] J. M. An and W. E. Pickett, Phys. Rev. Lett. **86**, 4366 (2001).
- [8] Y. Kong *et al.*, Phys. Rev. B **64**, 020501(R) (2001).
- [9] J. P. Carbotte, Rev. Mod. Phys. **62**, 1027 (1990).
- [10] ^{10}B absorbs neutrons too strongly for scattering measurements.
- [11] T. J. Sato, K. Shibata, and Y. Takano, cond-mat/0102468.
- [12] U. Buchenau *et al.*, Phys. Rev. B **34**, 5665 (1986). Although this paper deals with amorphous materials, the same formalism applies to coherently scattering polycrystals.
- [13] Since our original submission, another neutron measurement of the PDOS by T. Yildirim *et al.* (cond-mat/0103469) also shows no evidence of the 17 meV peak.
- [14] J. D. Jorgensen, D. G. Hinks, and S. Short, Phys. Rev. B **63**, 224522 (2001); cond-mat/0103069.
- [15] G. Eckold, M. Stein-Arsic, and H.-J. Weber, *UNISOFT—A Program Package for Lattice-Dynamical Calculations: User Manual* (IFF KFA, Jülich, 1986), Jül-Spez-366.
- [16] P. B. Allen and R. C. Dynes, Phys. Rev. B **12**, 905 (1975).